



GE Energy

David H. Hinds
Manager, ESBWR

PO Box 780 M/C L60
Wilmington, NC 28402-0780
USA

T 910 675 6363
F 910 362 6363
david.hinds@ge.com

MFN 05-166

Docket No. 52-010

December 19, 2005

U.S. Nuclear Regulatory Commission
Document Control Desk
Washington, D.C. 20555-0001

Subject: **NEDO-33081, Revision 1, "ESBWR Test Report," December 2005**

Enclosure 1 contains the subject topical report. This report is the non-proprietary version of NEDC-33081P, Revision 1, "ESBWR Test Report," May 2005, which was submitted in the Reference 1 letter.

If you have any questions about the information provided here, please let me know.

Sincerely,

A handwritten signature in black ink that reads "D.H. Hinds for".

David H. Hinds
Manager, ESBWR

D068

MFN 05-166

Page 2 of 2

Reference:

1. MFN 05-046, Robert E. Gamble to U.S. Nuclear Regulatory Commission, *GE Licensing Topical Report NEDC-33081P, Revision 1 "ESBWR Test Report," May 2005, May 27, 2005*

Enclosure:

1. MFN 05-166 – NEDO-33081, Revision 1, *ESBWR Test Report*, December 2005

cc: WD Beckner USNRC (w/o enclosure)
AE Cabbage USNRC (with enclosure)
LA Dudes USNRC (w/o enclosure)
GB Stramback GE San Jose (with enclosure)
eDRF 0000-0049-1573

MFN 05-166
Enclosure 1

ENCLOSURE 1

MFN 05-166

**NEDO-33081, Revision 1,
“ESBWR Test Report,” December 2005**



GE Nuclear Energy

NEDO-33081
Revision 1
Class I
eDRF 0000-0049-1573
December 2005

ESBWR Test Report

J.R. Fitch
T. Bandurski
Y.K. Cheung
J. Dreier
R.E. Gamble
J.M. Healzer
M. Huggenberger

NON PROPRIETARY INFORMATION NOTICE

This document is the non proprietary version of NEDC-33081P, Revision 1. Proprietary information which has been extracted is indicated by a vertical line in the right margin of the document. The attachments have been deleted in their entirety.

**IMPORTANT NOTICE REGARDING
CONTENTS OF THIS REPORT
PLEASE READ CAREFULLY**

Neither the General Electric Company nor any of the contributors to this document:

a. Makes any warranty or representation, express or implied, with respect to the accuracy, completeness, or usefulness of the information contained in this document, or that the use of any information, apparatus, method, or process disclosed in this document may not infringe privately owned rights;

or

b. Assumes any liabilities, including but not limited to nuclear liability, with respect to the use of, or for damages resulting from the use of any information, apparatus, method, or process disclosed in this document.

This work was performed partially as part of a contract between various utilities and GE for "ESBWR Development".

CHANGES FROM REV. 0

Some of the GENE responses to NRC requests for additional information (RAIs) committed to the revision of certain sections of NEDC-33081P. In addition, subsequent to the issue of Rev. 0 of NEDC-33081P, it was discovered that the PANDA instrumentation tables (Tables 2-1 to 2-7) required revision for consistency with the PANDA P-series test reports issued by the Paul Scherer Institute and to correct a typographical error. This resulted in an expansion of the original set of seven tables into a new set consisting of Tables 2-1 through 2-10. The "List of Tables" at the beginning of the report and the table references in the text were changed accordingly. The RAI-related changes and the additional revisions are incorporated herein and are denoted by "bars" in the left-hand margins of the affected paragraphs and tables (as shown to the left of this paragraph). Each of the RAI-related changes is further identified by a footnote that references the specific RAI that necessitated the change.

1. INTRODUCTION	1-1
2. PANDA P-SERIES TRANSIENT TESTS	2-1
2.1 Test Objectives	2-1
2.2 Test Description	2-1
2.3 Test Matrix	2-2
2.3.1 Test P1 (Base case) and Test P8 (Pool boildown)	2-2
2.3.2 Test P2 (Early start)	2-3
2.3.3 Test P3 (DW and PCCS initially filled with noncondensable)	2-3
2.3.4 Tests P4 and P5 (Delayed release of DW noncondensable)	2-4
2.3.5 Test P6 (ICS/PCCS interaction and VB leakage)	2-4
2.3.6 Test P7 (Lighter-than-steam noncondensable)	2-5
2.4 P-Series Test Results	2-5
2.4.1 Test P1/8	2-5
2.4.2 Test P2	2-6
2.4.3 Test P3	2-6
2.4.4 Test P4	2-6
2.4.5 Test P5	2-7
2.4.6 Test P6	2-7
2.4.7 Test P7	2-7
2.5 Summary and Conclusions	2-8
3. INTEGRATION OF TESTS	3-1
3.1 Comparison of PANDA P-Series Containment Pressures	3-1
3.2 WW Pressure vs. Increase in Noncondensable Mass	3-2
3.3 Summary of Containment Behavior	3-2
3.4 References	3-2

Attachments

List of Tables

Table 2-1	PANDA Flow Instrumentation	2-9
Table 2-2	PANDA RPV Power, Pressure and Temperature Instrumentation	2-9
Table 2-3	PANDA DW Pressure and Temperature Instrumentation	2-10
Table 2-4	PANDA WW Pressure and Temperature Instrumentation	2-10
Table 2-5	PANDA PCC Temperature Instrumentation	2-11
Table 2-6	PANDA IC Temperature Instrumentation	2-12
Table 2-7	PANDA Main Vent Temperature Instrumentation	2-12
Table 2-8	PANDA DW and WW Oxygen Probe Instrumentation	2-13
Table 2-9	PANDA Level Instrumentation	2-13
Table 2-10	PANDA Vent Phase and VB Open/Close Instrumentation	2-14
Table 2-11	PANDA Measurement Uncertainties	2-14

List of Figures

Figure 2-1	Isometric View of the PANDA Facility	2-15
Figure 2-2	Schematic of PANDA Test Facility	2-16
Figure 3-1	Comparison of DW Pressure for PANDA P-Series Tests	3-3
Figure 3-2	WW Pressure Increase versus Increase in Noncondensable Partial Pressure	3-4

1. INTRODUCTION

A comprehensive experimental program was previously carried out to provide data to qualify the TRACG computer code for analysis of the SBWR and to demonstrate the thermal-hydraulic performance of the systems and components in the original SBWR design. A subsequent test program, described herein, was carried out to provide additional test data to qualify the TRACG code and to assess the performance of the modified configuration and higher power level of the ESBWR. The SBWR tests have been documented in numerous test reports and a summary report that provides an integrated view of the SBWR test results from various scaled facilities. This report contains the additional test reports for the ESBWR and an integrated view of the scaled tests supporting the ESBWR design for post-accident containment pressure.

The objective of the SBWR test program was to provide test data to qualify the TRACG computer code for analysis of the SBWR and to validate the performance of the passive safety systems, namely:

- The Gravity-Driven Cooling System (GDCCS), which during a postulated loss-of-coolant accident (LOCA), supplies makeup water to the reactor core from a pool located above the core;
- The Isolation Condenser System (ICS), which during an isolation transient, uses natural circulation to remove core decay heat from the reactor pressure vessel (RPV) by condensing steam from the RPV and returning condensate to the RPV;
- The Passive Containment Cooling System (PCCS), which during a postulated LOCA, removes heat from the containment by condensing drywell steam and returning the condensate to the RPV.

Major SBWR test programs were conducted at the GIST, GIRAFFE, PANDA and PANTHERS test facilities at sites in the USA, Japan, Switzerland and Italy, respectively. GIST, GIRAFFE and PANDA were integral systems tests focusing on various aspects of the SBWR response to LOCAs. The PANTHERS tests were full-scale component tests of prototypical ICS and PCCS condensers.

The ESBWR design and technology program was started by GE to develop a passive BWR plant design combining the passive safety features of the 670-MWe SBWR with further innovations to improve the overall plant economics while maintaining or increasing the large performance margins. The original test and analysis activities for the SBWR design were completed in 1997. No additional testing and analysis were deemed necessary to support the 1390-MWe ESBWR plant design because the design uses the same basic features and components as the SBWR. The ESBWR design innovations were incorporated to increase margins while taking advantage of the economies of scale.

A significant ESBWR design modification, incorporated to increase containment pressure margins, was to connect the GDCCS gas space to the wetwell gas space rather than to the drywell gas space as it had been in the SBWR. This innovation provides a larger repository for the noncondensable gas that is swept from the drywell to the wetwell during the blowdown and

thereby reduces the post accident containment pressure. It was apparent that the large-scale PANDA test facility in Switzerland would be suitable for a confirmatory evaluation of the ESBWR response to a LOCA with the GDCS design modification. It also provided the opportunity to follow up on the significant conclusions from SBWR testing in PANDA that the PCCS system design had excessive heat removal capacity during the post blowdown period. Additional testing at PANDA would provide the means to evaluate the concept of allowing the PCCS pools to boil down below the elevation of the upper headers in the latter stages of the post-LOCA cooling transient. Accordingly, the PANDA facility was modified to represent the ESBWR GDCS configuration and the scaling was adjusted in accordance with the higher ESBWR decay heat load. A test matrix consisting of eight tests and designated the P-series was defined and the testing performed. The PANDA P-series test program is described in Section 2 of this report.

Section 3 of this reports covers testing integration. This section examines the testing of key phenomena at various scales and includes results from the ESBWR PANDA P-series tests. The inclusion of these data expands the qualification basis for the TRACG code.

2. PANDA P-SERIES TRANSIENT TESTS

2.1 Test Objectives

The PANDA P-series tests were performed as a joint effort by GE and the Paul Scherrer Institute (PSI) in Wuerenlingen, Switzerland. The objectives of the PANDA P-series test program were:

1. Reinforce the existing database for confirmation of the capability of TRACG to predict ESBWR containment system performance, including potential systems interaction effects.
2. Confirm the performance of the ESBWR containment configuration with the gas space of the gravity-drain cooling system (GDCCS) connected to the wetwell (WW) gas space.

Attachments 1 through 7 contain the P-series test reports issued by PSI. The following paragraphs supplement these reports with summary descriptions of the test facility, test matrix and test results.

2.2 Test Description

Figure 2-1 shows an isometric view of the PANDA facility. PANDA is a large-scale integrated containment structure originally designed to model the long-term cooling phase of the loss-of-coolant accident (LOCA) for the SBWR. It includes all the major components necessary to simulate containment system response during the long-term phase of a LOCA. It is a modular facility with separate pressure vessels representing the reactor pressure vessel (RPV), drywell (DW), wetwell (WW) and GDCCS pool. The reactor pressure vessel (RPV) is equipped with electrical heaters and heater controls to simulate decay heat and the release of RPV stored energy. The facility includes three scaled PCC heat exchangers and one isolation condenser (IC) unit and their associated water pools. Other components represented in PANDA include the vacuum breakers (VBs) between the DW and the WW and the equalization line (EQL) between the suppression pool and the RPV.

The RPV is represented by a single vessel in PANDA, while the DW and WW are represented by pairs of vessels, connected by large pipes. This double-vessel arrangement permits simulation of spatial distribution effects within the containment volumes. The water in the RPV is heated by a bank of controlled electrical heaters that can be programmed to match the decay heat curve. Main steam lines (MSLs) convey boiloff steam from the RPV to the two DW vessels. The PCC and IC inlet lines are connected to the DW and RPV vessels, respectively. Drain lines from the lower headers of the PCCs and IC return condensate to the RPV. Vent lines from the lower headers of the PCCs and the upper and lower headers of the IC connect at prototypical submergences in the suppression pools (SPs). Vacuum breakers (VBs) were installed in the lines connecting the DW and WW gas spaces. PANDA has the capability to valve out one of the MSLs, the IC and individual PCCs. It also has the capability to inject noncondensable gas (air or helium) into the DW over prescribed time periods during the post-LOCA transient simulation.

In the original PANDA/SBWR configuration, the GDCS gas space was connected to the DW. A major alteration of PANDA for the ESBWR was to connect the GDCS gas space to the WW gas space. This ESBWR design modification provides a larger repository for the noncondensable gas that is swept from the DW to the WW during the blowdown and thereby reduces the containment pressure. In its original configuration, PANDA was a 1/25 volume-scaled, full-height simulation of the SBWR primary system and containment. As configured for the P-series tests, the PANDA facility is a full-height simulation of the ESBWR containment at a nominal volumetric scale of 1:45. The piping interconnecting the PANDA vessels is scaled (primarily with the use of orifice plates) to produce the same pressure loss as the corresponding ESBWR piping at the scaled flow rate. The three PANDA PCC units are approximately equivalent to the four ESBWR PCC units and the one PANDA IC unit is about 10% underscaled relative to the four ESBWR IC units. Figure 2-2 shows a schematic of the PANDA facility with the test vessels and their interconnecting piping in the base-case configuration for the P-series tests.

2.3 Test Matrix

The P-series test matrix consisted of eight tests to investigate various aspects of the long-term cooling phase following a guillotine rupture in one of the ESBWR main steam lines (MSLB). The eight P-series tests covered a wide range of PCCS startup and operating conditions. The P-series tests also addressed system interaction effects involving the various passive systems and components that play a role in the ESBWR containment response to a LOCA. In addition to the PCCS, these systems and components include the ICS, GDCS and VBs. The P-series tests included cases with both symmetric and asymmetric steam flow to the two DW vessels and cases involving the delayed release of a noncondensable gas (air or helium) within the DW. Finally, the P-series tests considered several extreme conditions, including PCCS startup with the DW filled with air, DW-to-WW bypass leakage and elimination of one PCC loop. A detailed description of the facility configuration, initial conditions and operator actions for each of the P-series tests is given in the PSI test reports (Attachments 1 through 7). Tables 2-1 through 2-10 describe the PANDA instrumentation referenced in the test reports. The figure numbers in the first column of these tables correspond to the figure numbers in the test reports. Table 2-11 shows the PANDA measurement uncertainties. The facility configuration, initial conditions and rationale for each of the tests are summarized below.

2.3.1 Test P1 (Base case) and Test P8 (Pool boildown)

The base case (Test P1) was a simulation of the long-term cooling phase following a LOCA caused by a guillotine rupture of one of the main steam lines. This LOCA scenario leads to the highest long-term containment pressure in the ESBWR. Test P1 had equal steam flow from the RPV to each of the two PANDA DW vessels and all three PCC units in service. The initial conditions were comparable to ESBWR conditions at about one hour from the occurrence of the LOCA. Test P8 was performed as an extension of Test P1 that examined PCCS performance with boildown of the condenser pools below the bottom of the condenser upper headers. The combination of Tests P1 and P8 is designated as Test P1/8

2.3.2 Test P2 (Early start)

Test P2 examined PCCS performance during the portion of the post-LOCA transient extending from the early GDCS injection phase into the long-term cooling phase. At the end of the blowdown (marked by the start of GDCS injection and the cessation of flow through the main LOCA vents), the PCC units are operating at relatively high power in an essentially pure-steam environment. As GDCS injection proceeds, steam flow from the RPV to the DW is reduced and the DW pressure begins to fall. The decreasing DW pressure reduces the flow to the PCCS. Eventually, the decreasing DW pressure opens the VBs and allows the return of noncondensable gas to the DW. As the rate of GDCS injection decreases and the RPV inventory heats up to saturation, the DW re-pressurizes and flow to the PCCS resumes. This marks the initiation of the long-term cooling phase.

By simulating the portion of the post-LOCA transient described above, Test P2 addressed the behavior of the PCCS under conditions covering the range from high-power operation with pure-steam inlet conditions, flow reduction caused by decreasing DW pressure, resumption of flow caused by increasing DW pressure, degraded heat transfer with steam-air inlet conditions, and, finally, return to operation under the full decay heat load. It further addressed systems interactions between the PCCS, GDCS, and the VBs.

2.3.3 Test P3 (DW and PCCS initially filled with noncondensable)

The main purpose of Test P3 was to address the issue of PCCS startup and operation from a condition representing the upper limit of initial DW noncondensable inventory. The ESBWR LOCA analysis shows that essentially the entire initial inventory of the DW inerting gas is forced into the WW during a period of time much shorter than the reactor blowdown period.¹ Thus, when the ESBWR PCCS is called upon to assume the decay heat load, it is expected that it will face a minimal challenge from residual noncondensable gas in the inlet mixture. It is possible for gas to "hide out" in various dead-end regions of the DW and subsequently find its way to the PCCS inlet lines, but this is a long-term process which would not be expected to interfere with initial PCCS operation at high decay heat load.

¹ Revised in response to RAI 346.1

A secondary purpose of Test P3 was to simulate the effect of steam flowing preferentially to one side of the DW in the ESBWR by forcing all of the RPV steam to flow to DW2 and by valving out the PCC unit (PCC1) attached to DW1. A major design objective of the PCCS is that the system should be "robust" in the sense of being able to adjust to a wide range of inlet conditions, including those associated with nonuniform distributions of steam and noncondensable gas in the DW. Directing all the RPV steam to DW2 and shutting off the PCC unit on DW1 creates the maximum degree of asymmetry in the PANDA DW. Shutting off one PCC unit and running at constant power simultaneously puts the PCCS in an overload condition. The combination of asymmetric steam flow, limiting initial DW noncondensable inventory and PCCS overload addresses the objective of a robust PCCS.

2.3.4 Tests P4 and P5 (Delayed release of DW noncondensable)

Tests P4 and P5 further address the issue of PCCS robustness by considering the effect of a delayed release of noncondensable gas from DW "hideout" regions where it may have been trapped during the initial blowdown and subsequent PCCS purging. The initial conditions for both Tests P4 and P5 are the same as for the Base case Test P1. At four hours from test initiation, air was injected to DW1 for 30 min. Test P5 differed from Test P4 by having one of the two PCCs (PCC2) on DW2 shut off. These tests demonstrated PCCS performance when the system has been operating in balance with the RPV heat load and is abruptly forced to deal with the degrading effect of noncondensable in the inlet flow. Test P5 increases the challenge by having one of the PCC units out of service. Finally, Test P4 serves as a repeat of the base case Test P1 for the four hours that precede the air injection.

2.3.5 Test P6 (ICS/PCCS interaction and VB leakage)

Test P6 considered system interaction effects associated with parallel operation of the ICS and PCCS and the effect of a direct bypass of steam from the DW to the WW air space. Both of these effects are directly applicable to design-basis evaluation of PCCS performance following a postulated LOCA in the ESBWR. In the ESBWR, the ICS would automatically come into operation on a low RPV water level signal and would immediately start condensing RPV steam, operating in parallel with the PCCS. The only uncertainty is whether the IC vents to the WW would be opened because this operation must be performed by the operator. Not opening the vent might cause ICS shutdown from accumulation of noncondensable. To cover this possibility in Test P6, the IC was valved out of service after seven hours of operation. This guaranteed that the test would address the situation in which, after an initial period of IC operation, the decay heat load must be shifted from the ICS to the PCCS.

2.3.6 Test P7 (Lighter-than-steam noncondensable)

Test P7 investigated PCCS performance under a challenging set of circumstances that might be associated with a severe accident scenario. The initial conditions were as predicted for the ESBWR at one hour from the instant of the LOCA. An asymmetric overload condition was set up by releasing all of the RPV steam to DW2 and by valving out the PCC unit (PCC1) on DW1. At four hours from test initiation, helium was injected to DW1 for a period of two hours. This presented the PCCS with the dual challenge of dealing with the delayed release of a lighter-than-steam noncondensable gas while in an overload condition.

2.4 P-Series Test Results

Attachments 1 through 7 contain a comprehensive set of Figures showing the transient behavior of key variables for each of the P-series tests. The figures are accompanied by a "Main Observations" section that describes the important phenomena observed during the test. These observations are summarized below.

2.4.1 Test P1/8

2.4.2 Test P2

2.4.3 Test P3

2.4.4 Test P4

2.4.5 Test P5

2.4.6 Test P6

2.4.7 Test P7

2.5 Summary and Conclusions

**Table 2-1
PANDA Flow Instrumentation**

Figure No.	Instrument ID	Measurement
3	MV.MS1	Steam flow to DW1
3	MV.MS2	Steam flow to DW2
4	MV.P1F	PCC1 inlet flow
4	MV.P2F	PCC2 inlet flow
4	MV.P3F	PCC3 inlet flow
4	MV.I1F	IC inlet flow
5	MV.I1C	Total (ICS and PCCS) drain flow to RPV
22	MM.BOG	Air flow to DW1
22	MM.B2E	Helium flow to DW1
22	MV.VL1	Bypass leakage flow

**Table 2-2
PANDA RPV Power, Pressure and Temperature Instrumentation**

Figure No.	Instrument ID	Measurement
2	MW.RP.7	RPV heater power
1	MP.RP.1	RPV dome pressure
6	MTF.RP.1	RPV fluid temperature 14.5m from bottom
6	MTF.RP.2	RPV fluid temperature 12.8m from bottom
6	MTF.RP.3	RPV fluid temperature 11.1m from bottom
6	MTF.RP.4	RPV fluid temperature 2.0m from bottom
6	MTF.RP.5	RPV fluid temperature 0.1m from bottom

**Table 2-3
PANDA DW Pressure and Temperature Instrumentation**

Figure No.	Instrument ID	Measurement
1	MP.D1	DW1 pressure
7	MTG.D1.1	DW1 vapor temperature, 7.11m from tank bottom
7	MTG.D1.2	DW1 vapor temperature, 5.78m from tank bottom
7	MTG.D1.3	DW1 vapor temperature, 4.46m from tank bottom
7	MTG.D1.4	DW1 vapor temperature, 3.13m from tank bottom
7	MTG.D1.5	DW1 vapor temperature, 1.81m from tank bottom
7	MTG.D1.6	DW1 vapor temperature, 0.48m from tank bottom
8	MTG.D2.1	DW2 vapor temperature, 7.11m from tank bottom
8	MTG.D2.2	DW2 vapor temperature, 5.78m from tank bottom
8	MTG.D2.3	DW2 vapor temperature, 4.46m from tank bottom
8	MTG.D2.4	DW2 vapor temperature, 3.13m from tank bottom
8	MTG.D2.5	DW2 vapor temperature, 1.81m from tank bottom
8	MTG.D2.6	DW2 vapor temperature, 0.48m from tank bottom

**Table 2-4
PANDA WW Pressure and Temperature Instrumentation**

Figure No.	Instrument ID	Measurement
1	MP.S1	WW1 pressure
9	MTG.S1.1	WW1 vapor temperature, 9.53m from tank bottom
9	MTG.S1.3	WW1 vapor temperature, 7.63m from tank bottom
9	MTG.S1.6	WW1 vapor temperature, 4.03m from tank bottom
10	MTG.S2.1	WW2 vapor temperature, 9.52m from tank bottom
10	MTG.S2.3	WW2 vapor temperature, 7.62m from tank bottom
10	MTG.S2.6	WW2 vapor temperature, 4.02m from tank bottom
9	MTL.S1.1	WW1 liquid temperature, 3.53m from tank bottom
9	MTL.S1.6	WW1 liquid temperature, 1.03m from tank bottom
10	MTL.S2.1	WW2 liquid temperature, 3.52m from tank bottom
10	MTL.S2.6	WW2 liquid temperature, 1.02m from tank bottom
9	MTS.S1.1	WW1 liquid temperature just below pool surface
10	MTS.S2.1	WW2 liquid temperature just below pool surface

**Table 2-5
PANDA PCC Temperature Instrumentation**

Figure No.	Instrument ID	Measurement
11a	MTG.P1.1	PCC1 upper header vapor temperature
11b	MTG.P1.2	PCC1 lower header vapor temperature
11a	MTG.P1.3	PCC1 tube vapor temperature, 0.81m above tube center
11a	MTG.P1.4	PCC1 tube vapor temperature, 0.61m above tube center
11a	MTG.P1.5	PCC1 tube vapor temperature, 0.41m above tube center
11b	MTG.P1.6	PCC1 tube vapor temperature, 0.20m above tube center
11b	MTG.P1.7	PCC1 tube vapor temperature at tube center
11b	MTG.P1.8	PCC1 tube vapor temperature, 0.41m below tube center
11b	MTG.P1.9	PCC1 tube vapor temperature, 0.81m below tube center
12a	MTG.P2.1	PCC2 upper header vapor temperature
12b	MTG.P2.2	PCC2 lower header vapor temperature
12a	MTG.P2.3	PCC2 tube vapor temperature, 0.81m above tube center
12a	MTG.P2.4	PCC2 tube vapor temperature, 0.61m above tube center
12a	MTG.P2.5	PCC2 tube vapor temperature, 0.41m above tube center
12b	MTG.P2.6	PCC2 tube vapor temperature, 0.20m above tube center
12b	MTG.P2.7	PCC2 tube vapor temperature at tube center
12b	MTG.P2.8	PCC2 tube vapor temperature, 0.41m below tube center
12b	MTG.P2.9	PCC2 tube vapor temperature, 0.81m below tube center
13a	MTG.P3.1	PCC3 upper header vapor temperature
13b	MTG.P3.2	PCC3 lower header vapor temperature
13a	MTG.P3.3	PCC3 tube vapor temperature, 0.81m above tube center
13a	MTG.P3.4	PCC3 tube vapor temperature, 0.61m above tube center

Table 2-5 (continued)
PANDA PCC Temperature Instrumentation

13a	MTG.P3.5	PCC3 tube vapor temperature, 0.41m above tube center
13b	MTG.P3.6	PCC3 tube vapor temperature, 0.20m above tube center
13b	MTG.P3.7	PCC3 tube vapor temperature at tube center
13b	MTG.P3.8	PCC3 tube vapor temperature, 0.41m below tube center
13b	MTG.P3.9	PCC3 tube vapor temperature, 0.81m below tube center

**Table 2-6
PANDA IC Temperature Instrumentation**

Figure No.	Instrument ID	Measurement
23a	MTG.I1.1	IC upper header vapor temperature
23b	MTG.I1.2	IC lower header vapor temperature
23a	MTG.I1.3	IC tube vapor temperature, 0.81m above tube center
23a	MTG.I1.4	IC tube vapor temperature, 0.61m above tube center
23a	MTG.I1.5	IC tube vapor temperature, 0.41m above tube center
23b	MTG.I1.6	IC tube vapor temperature, 0.20m above tube center
23b	MTG.I1.7	IC tube vapor temperature at tube center
23b	MTG.I1.8	IC tube vapor temperature, 0.41m below tube center
23b	MTG.I1.9	IC tube vapor temperature, 0.81m below tube center

**Table 2-7
PANDA Main Vent Temperature Instrumentation**

Figure No.	Instrument ID	Measurement
20a	MTG.MV1.1	Main vent 1 inlet temperature
20a	MTG.MV1.2	Main vent 1 temperature at entrance to WW1
20a	MTG.MV1.3	Main vent 1 temperature, 2.82m above vent exit
20a	MTG.MV1.4	Main vent 1 temperature, 0.03m above vent exit
20b	MTG.MV2.1	Main vent 2 inlet temperature
20b	MTG.MV2.2	Main vent 2 temperature at entrance to WW2
20b	MTG.MV2.3	Main vent 2 temperature, 2.82m above vent exit
20b	MTG.MV2.4	Main vent 2 temperature, 0.03m above vent exit

**Table 2-8
PANDA DW and WW Oxygen Probe Instrumentation**

Figure No.	Instrument ID	Measurement
14	MPG.D1.1	DW1 air partial pressure, 6.8m from tank bottom
14	MPG.D1.2	DW1 air partial pressure, 3.1m from tank bottom
14	MPG.D1.3	DW1 air partial pressure, 0.9m from tank bottom
14	MPG.D2.1	DW2 air partial pressure, 6.8m from tank bottom
14	MPG.D2.2	DW2 air partial pressure, 3.1m from tank bottom
14	MPG.D2.3	DW2 air partial pressure, 0.9m from tank bottom
15	MPG.S1	WW1 air partial pressure, 9.2m from tank bottom
15	MPG.S2	WW2 air partial pressure, 9.2m from tank bottom

**Table 2-9
PANDA Level Instrumentation**

Figure No.	Instrument ID	Measurement
16	ML.U1	PCC1 pool level
16	ML.U2	PCC2 pool level
16	ML.U3	PCC3 pool level
16	ML.U0	IC pool level
17	ML.RP.1	RPV collapsed level
17	ML.GD	GDCS collapsed level

Table 2-10
PANDA Vent Phase and VB Open/Close Instrumentation

Figure No.	Instrument ID	Measurement
18a	MI.P1V.1	Phase indicator at PCC1 vent exit
18b	MI.P2V.1	Phase indicator at PCC2 vent exit
18c	MI.P3V.1	Phase indicator at PCC3 vent exit
19a	MI.MV1	Phase indicator at main vent 1 exit
19b	MI.MV2	Phase indicator at main vent 2 exit
21a	CB.VB1	VB1 open/close indicator
21b	CB.VB2	VB2 open/close indicator

Table 2-11
PANDA Measurement Uncertainties

Measurement	Maximum Uncertainty
Temperature	$\pm 0.8^{\circ}\text{C}$
Pressure	$\pm 2.3 \text{ kPa}$
Flow	$\pm 2\%$
Air Partial Pressure	$\pm 4\%$
PCC/IC Pool Level	$\pm 0.156\text{m}$

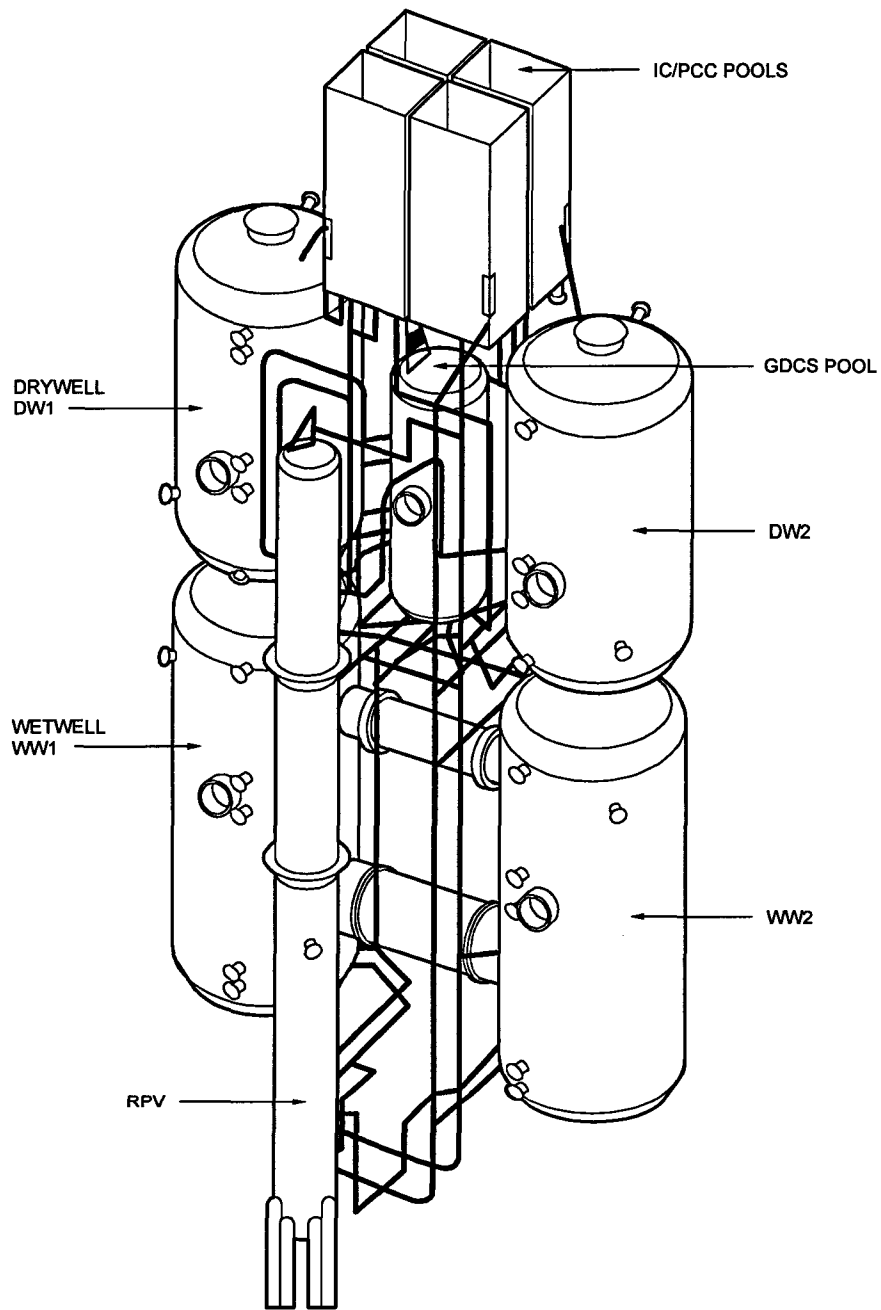


Figure 2-1. Isometric View of the PANDA Facility

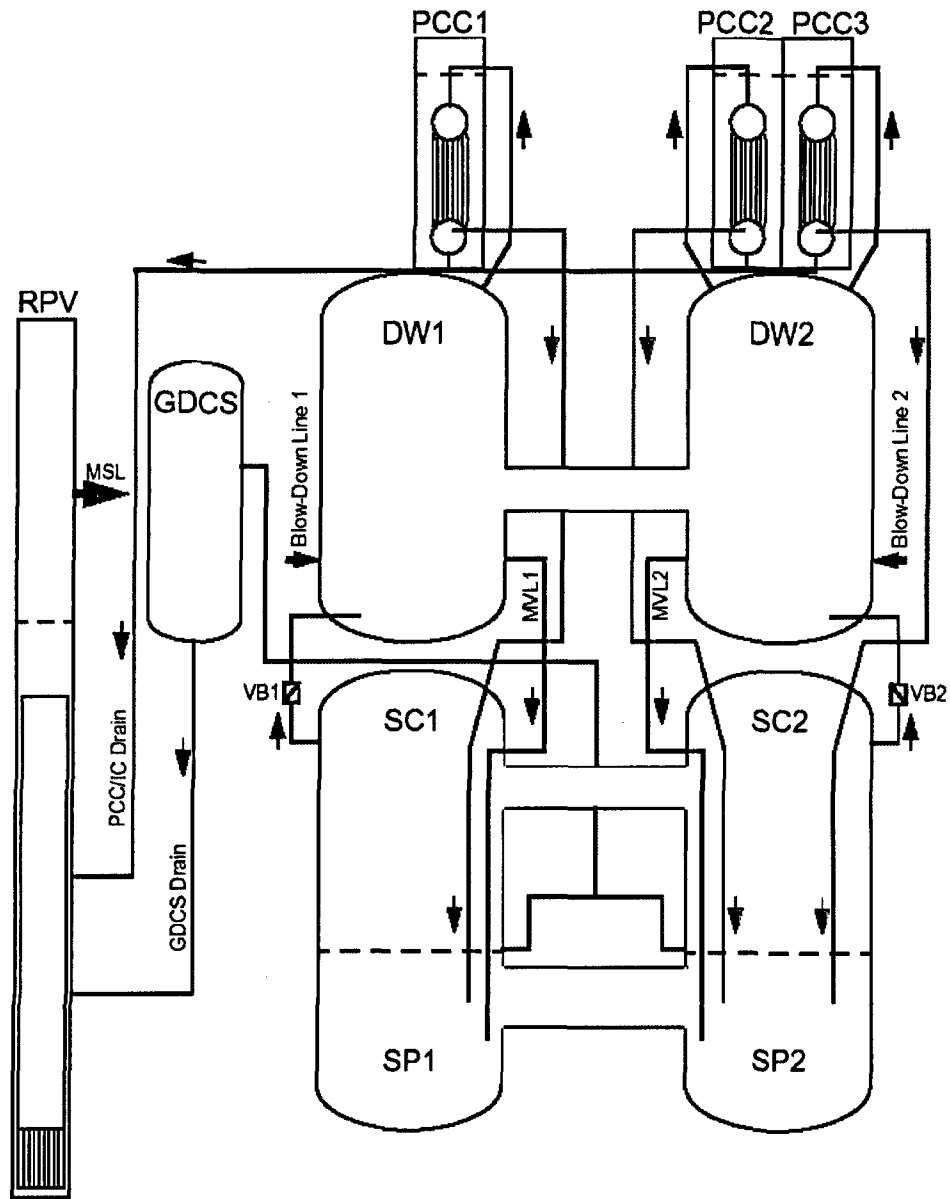


Figure 2-2. Schematic of PANDA Test Facility

3. INTEGRATION OF TESTS

The SBWR Testing Summary Report [3-1] contained an extensive discussion of scaling issues related to the SBWR test program and relevant comparisons of results obtained from test facilities at different scales. This section updates two of the specific comparisons from Reference 3-1. The first demonstrates the consistency of the post-LOCA containment pressures from three of the PANDA P-series tests. The second comparison adds results from two of the PANDA P-series tests to a figure from Reference 3-1 showing how the long-term increase in wetwell pressure can be related to the increase in wetwell noncondensable inventory for tests covering a wide range of scales.

3.1 Comparison of PANDA P-Series Containment Pressures

Long-term containment performance involves removal of decay heat while assuring that the containment pressure and temperature remain below their design limits. The PANDA P-series tests provided data that are applicable to ESBWR long-term containment performance. This section provides long-term pressure comparisons from three PANDA P-series tests.

The PANDA P-series tests selected for comparison are Tests P1, P2 and P4. Test P1 is the base case with initial conditions comparable to the design evaluation of the ESBWR main steam line break at one hour from the start of the LOCA. Test P4 (prior to the drywell air injection) was a repeat of the base case. The initial conditions for Test P2 were chosen to represent the end of the GDCS injection phase (approximately 20 minutes from the start of the LOCA). Figure 3-1 compares the measured drywell pressures from the three tests. The origins of the time scales have been adjusted to approximately match the corresponding times in the ESBWR post-LOCA transient.

Figure 3-1 shows the drywell pressure transient associated with the movement of residual noncondensable back to the WW, the clearing of noncondensable from the PCC units and the balancing of the PCCS heat removal with the RPV heat load. For both Tests P1 and P4, this initial transient is repeated following the opening of a vacuum breaker. Eventually, the PCCS balances the RPV heat load and an equilibrium condition is established. Test P2 shows generally the same type of transient behavior. The pressure initially decreases because the draining of the GDCS causes an immediate vacuum breaker opening that returns some of the initial wetwell noncondensable to the drywell. The pressure increase that follows is very similar to that observed in Tests P1 and P4 but does not quite reach the pressure peak observed in the other two tests. Test P2 was also affected by leakage through the check valve in the GDCS line that resulted in two subsequent GDCS-draining transients and an accompanying suppression of RPV steaming. It appears that Test P2 was on the verge of a second vacuum breaker opening when the test ended and it is expected that the ensuing transient would have led to an equilibrium pressure close to that in the other two tests.

3.2 WW Pressure vs. Increase in Noncondensable Mass

The dependence of the WW pressure on the increase in noncondensable mass is shown in Figure 3-2 where the total pressure increase in the WW is plotted against the measured noncondensable partial pressure increase. The values are normalized by the average of the initial and final WW pressures for each test. Points are plotted for PANDA M-series Tests M3 and M7, GIRAFFE Tests H1, H2, H3 and H4 [3-2] and PANDA P-series Tests P3 and P4. Points falling on the 45-degree line in this figure would indicate that the wetwell pressure change was exactly equal to the increase in noncondensable partial pressure. As discussed in Reference 3-1, the points fall very close to this line, indicating that the transport of noncondensables to the WW is the predominant cause of the WW pressure increase. The results for the two P-series tests are very close to the 45-degree line and are consistent with the results from the earlier SBWR integral systems tests in both the PANDA and the GIRAFFE test facilities.

3.3 Summary of Containment Behavior

The comparisons above support the conclusion that the phenomena important to long-term containment behavior were well represented in the PANDA P-series test facility. Although there are variations in the specific behavior due to the initialization and movement of noncondensables and the effect of GDCS injection on the RPV steaming rate, the overall behavior of the base-case and early-start P-series tests is similar. The P-series test matrix was sufficient to encompass the range of behaviors expected in the ESBWR. Inclusion of the P-series tests in the prior SBWR comparison of change in WW pressure vs. change in WW noncondensable partial pressure reinforces the conclusion that the increase in noncondensable is the predominant cause of the WW pressure increase. This comparison also indicates that the P-series tests did not introduce phenomena that had not been considered in the extensive scaling evaluation performed for the earlier SBWR test program.

3.4 References

- 3-1. NEDC-32606P, *SBWR Testing Summary Report* (Rev. B), November 1996.
- 3-2. NEDC-32725P, *TRACG Qualification for SBWR* (Rev. 1), August 2002.

Figure 3-1. Comparison of DW Pressures for PANDA P-Series Tests

Figure 3-2: WW Pressure Increase versus Increase in Noncondensable Partial Pressure

Attachments

1. M. Huggenberger, C. Aubert, T. Bandurski, J. Dreier, O. Fischer and H. J. Strassberger, *Integral System Tests P1 and P8 Test Report*, ALPHA-716-0, TM-42-97-19, Paul Scherrer Institut, 18. May 1998.
2. M. Huggenberger, C. Aubert, T. Bandurski, J. Dreier, O. Fischer and H. J. Strassberger, *Integral System Tests P2 Test Report*, ALPHA-816-0, TM-42-98-16, Paul Scherrer Institut, 26. May 1998.
3. M. Huggenberger, C. Aubert, T. Bandurski, J. Dreier, O. Fischer and H. J. Strassberger, *Integral System Tests P3 Test Report*, ALPHA-819-0, TM-42-98-19, Paul Scherrer Institut, 9. June 1998.
4. M. Huggenberger, C. Aubert, T. Bandurski, J. Dreier, O. Fischer and H. J. Strassberger, *Integral System Tests P4 Test Report*, ALPHA-821-0, TM-42-98-21, Paul Scherrer Institut, 25. June 1998.
5. M. Huggenberger, C. Aubert, T. Bandurski, J. Dreier, O. Fischer and H. J. Strassberger, *Integral System Tests P5 Test Report*, ALPHA-823-0, TM-42-98-24, Paul Scherrer Institut, 17. August 1998.
6. M. Huggenberger, C. Aubert, T. Bandurski, J. Dreier, O. Fischer and H. J. Strassberger, *Integral System Tests P6 Test Report*, ALPHA-827-0, TM-42-98-28, Paul Scherrer Institut, 17. August 1998.
7. M. Huggenberger, C. Aubert, T. Bandurski, J. Dreier, O. Fischer and H. J. Strassberger, *Integral System Tests P7 Test Report*, ALPHA-828-0, TM-42-98-29, Paul Scherrer Institut, 7. October 1998.

These Attachments are proprietary in their entirety and have been deleted from this document.